INTERNATIONAL JOURNAL FOR NUMERICAL METHODS IN FLUIDS
Int. J. Numer. Meth. Fluids 2005; **47**:895–902
Published online 21 January 2005 in Wiley InterScience (www.interscience.wiley.com). DOI: 10.1002/fld.896

Upwinding and implicit residual smoothing on cell-vertex unstructured grids

L. A. Catalano*,† and V. S. E. Daloiso‡

DIMeG, CEMeC—Politecnico di Bari, via Re David 200, I-70125 Bari, Italy

SUMMARY

A new line-search algorithm for cell-vertex unstructured triangular grids is proposed in this paper and combined with an implicit residual smoothing procedure, to accelerate convergence of a recently developed upwind finite-volume method for the Euler and the Navier–Stokes equations. Both the standard implementation with two smoothing lines and a new procedure using four directions are considered and fully tested to evaluate their efficiency and to determine the optimal smoothing parameters. Copyright © 2005 John Wiley & Sons, Ltd.

KEY WORDS: unstructured; line-search; residual smoothing

1. INTRODUCTION

Engineering applications often require the analysis of complex geometries, which can be easily discretized by means of unstructured meshes. Most methods for unstructured grids proposed to date employ a cell-vertex discretization, since it allows a natural definition of the cell-based flow gradients, which are required both for the higher-order reconstruction and for the discretization of the viscous terms. In the framework of a finite-volume approach, the authors have recently developed and validated a new higher-order accurate 2D and 3D gradient-based reconstruction to discretize the convective terms of the Navier–Stokes equations [1–3]. The reconstruction employs the same (cell-based) gradients needed for the discretization of the diffusive terms, with no additional averaging.

The natural further step is to implement a suitable technique that accelerates convergence to steady-state. One of the most successful techniques in use is the so-called implicit residual

*Correspondence to: L. A. Catalano, DIMeG, CEMeC—Politecnico di Bari, via Re David 200, I-70125 Bari, Italy.
†E-mail: catalano@poliba.it
‡E-mail: daloiso@imedado.poliba.it

Contract/grant sponsor: MIUR; contract/grant number: CEMeC, PRIN

Received 27 April 2004
Accepted 16 September 2004

smoothing (IRS), first introduced by Lerat [4] for the Lax–Wendroff scheme, and later extended by Jameson [5] to Runge–Kutta schemes. This technique enlarges the stability range of the basic time-stepping scheme allowing higher CFL numbers to be used. The technique is easily applied on structured grids, where the smoothing directions coincide with the grid-lines. However, its application on unstructured grids is not straightforward, since proper smoothing lines must be found. This paper proposes a new line-search (LS) algorithm for cell-vertex 2D unstructured triangular grids, which can be easily extended to three dimensions, and is characterized by another important feature: owing to the arbitrary choice of the LS direction, the smoothing procedure can be applied on more than two lines, thus resulting in a further convergence and robustness improvement. The paper will also present the results of an exhaustive numerical study on well-known inviscid and laminar test cases, to validate both the LS algorithm and the multi-direction smoothing, as well as to demonstrate the very high efficiency and robustness both for single-grid and multi-grid computations.

2. SPACE DISCRETIZATION

An unstructured cell-vertex triangular grid is used to discretize the 2D Euler and Navier–Stokes equations employed in this paper. A left state and a right state, $Q^{\mathrm{L}}_{(ij)}$ and $Q^{\mathrm{R}}_{(ij)}$, are reconstructed on the two sides of each interface (ij), obtained by connecting either the barycentres or the circumcentres of two neighbouring triangles. For the left state, one has

$$Q^{\mathrm{L}}_{(ij)} = Q_j + (\nabla Q)_{ji} \cdot \mathbf{l}_{ji} \tag{1}$$

$\mathbf{l}_{ji}$ being the vector pointing from the node j to the mid-point of the side; see Figure 1. Standard one-dimensional limiters can also be applied straightforwardly. It can be easily shown that in one dimension the reconstruction of the left state is based on the *gradient* of Q in the left-neighbouring cell. Similarly, in two and three dimensions, a unique left-neighbouring cell can be defined as the cell C_{ji}, which contains the prolongation of the side (ji), plotted as a dot–dashed line in Figure 1. The cell C_{ji} is searched only once and can be stored as a pointer (except in the case of moving grids). The choice of a cell-vertex triangular grid allows to compute the cell-based gradient $(\nabla Q)_{ji} \equiv (\nabla Q)_{C_{ji}}$ uniquely. All gradients must

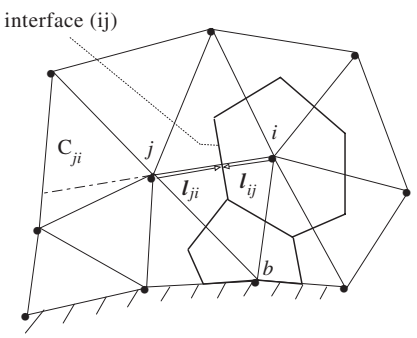

Figure 1. Higher-order reconstruction.

be computed once at each iteration, stored, and then used without any additional averaging. For this reason, and since the same gradients must be computed anyway when solving the Navier–Stokes equations, the authors claim that the proposed higher-order reconstruction minimizes the computational time required for the evaluation of the flow gradients [1–3]. The flux-difference-splitting of Roe [6] is then used to solve the Riemann problem defined at each interface. A standard finite-element Galerkin discretization is used for the viscous terms.

3. LINE-SEARCH ALGORITHM

Starting from a generic node (stored as $\ell = 1$ in the line), a smoothing line as close as possible to a generic direction $\mathbf{e}$ is recursively obtained as follows: consider all edges s containing the node ℓ and compute the scalar product $(\mathbf{s} \cdot \mathbf{e})$, $\mathbf{s}$ being the versor of s pointing from ℓ to its second node. The edge with maximum scalar product is chosen as connecting line: thus, the second node of that edge is stored as the node $(\ell + 1)$ of the line. Figure 2 illustrates this process for the particular case $\mathbf{e} \equiv \mathbf{i}$: three choices are possible, since backward-pointing edges can be *a priori* discarded. The scalar product is maximum for the edge s_2 which will be chosen as part of the smoothing line. This criterion allows to choose the edge aligned as much as possible with the chosen smoothing direction $\mathbf{e}$. The procedure is then applied to the subsequent node, so as to select a new edge of the connecting line. The search stops either when the boundary is reached or when all possible subsequent nodes already belong to pre-existent lines. When one of these events occurs, a new line can be started from the first *free* node of the grid. The process stops when all nodes of the grid belong to a line. Figure 2 also provides an example of the resulting line-pattern in the direction $\mathbf{e} \equiv \mathbf{i}$.

It may happen that the node selected as the subsequent one is the first node of an existing line. In such a case, the algorithm allows to join the forming line to the previous one, thus generating a unique longer line. This allows one to chose the starting nodes randomly.

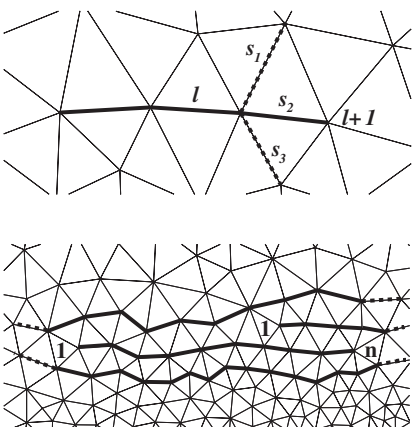

Figure 2. Line search in the x-direction.

At the end of the procedure, every node must belong to one line only. Lines can have any length, but one- and two-node lines are not allowed. If such lines are present, they are inserted in a longer line. A simple way to perform this junction is to cut a longer line and let the short line to be joined. The final pattern of lines will be only slightly deformed with no influence on the IRS technique.

4. RESIDUAL SMOOTHING AND MULTIGRID

The discretized governing equations are solved by means of a four-stage Runge–Kutta scheme: at each stage, the explicit residual $\mathscr{R}^{\mathrm{e}}$ is modified as [4, 5]

$$\mathscr{R}^i = \mathscr{R}^{\mathrm{e}} + \hat{\varepsilon}\nabla^2 \mathscr{R}^i \tag{2}$$

where $\mathscr{R}^i$ is the smoothed residual and $\hat{\varepsilon}$ is a suitable positive variable used to control the smoothing. To reduce the computational effort, Equation (2) is factorized and applied in N_{s} steps along the N_{s} smoothing directions $\mathbf{e}_k$:

$$\begin{gathered} \mathscr{R}^{(0)} = \mathscr{R}^{\mathrm{e}} \\ (1 - \varepsilon(\nabla\Delta)_{\mathbf{e}_k})\mathscr{R}^{(k)} = \mathscr{R}^{(k-1)}, \quad k = 1, \ldots, N_{\mathrm{s}} \\ \mathscr{R}^i = \mathscr{R}^{(N_{\mathrm{s}})} \end{gathered} \tag{3}$$

using a value of ε independent of $\mathbf{e}_k$, for simplicity. In Equation 3, $(\nabla\Delta)_{\mathbf{e}_k}$ is the standard second difference operator applied on each line corresponding to $\mathbf{e} = \mathbf{e}_k$. The standard application of the IRS procedure considers two smoothing directions aligned with the (structured) grid lines, and thus almost orthogonal. However, owing to the generality of the LS algorithm and due to the non-existence of a preferential direction on unstructured triangular grids, more than two smoothing directions can be usefully employed. Numerical experiments show that $N_{\mathrm{s}} = 4$ (with 45° between each direction) is sufficient to obtain an effective multi-directional smoothing and thus can be considered as the optimal choice.

A standard V-cycle full multigrid (FMG) [7] has been also implemented to accelerate convergence to steady state. Finer grids are created during the nested iteration by means of a global uniform refinement, improved by a grid-point adjustment.

5. RESULTS

Four well-known inviscid and laminar test-cases have been considered to validate the LS algorithm and the multi-direction IRS, as well as to suggest the optimal smoothing constants for each flow regime (inviscid/laminar, subsonic/transonic): (i) the inviscid subsonic flow in a 20% striction channel with outlet isoentropic Mach number $M_{2,\mathrm{is}} = 0.5$; (ii) the subsonic ($M_\infty = 0.5$) and (iii) the transonic ($M_\infty = 0.8$) inviscid flows past a NACA-0012 airfoil with incidence angle $\alpha = 1°$; (iv) the laminar flow past the same airfoil with incidence angle $\alpha = 10°$, $M_\infty = 0.8$ and $Re = 500$. Figures 3 and 4 provide the Mach number contours ($\Delta M = 0.05$) for the channel flow and for the inviscid transonic flow past the airfoil, respectively. Very fine grids (about 14 000 cells) have been employed in all applications to better

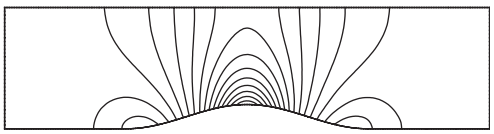

Figure 3. Channel flow.

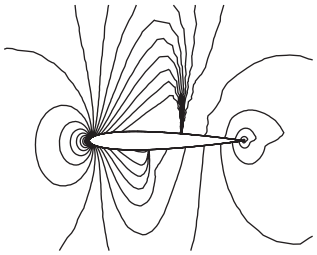

Figure 4. Inv. transonic airfoil.

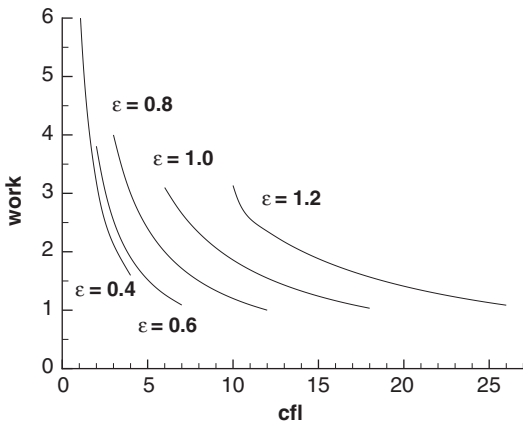

Figure 5. Channel flow: 4-line smoothing.

test both the LS and the IRS strategies, the accuracy of the space discretization already having been demonstrated in References [1–3].

Using different values of ε and CFL number, an exhaustive application of the code to the single-grid solution of the channel flow problem has been performed, both to find out the optimal parameters and to compare the efficiency of the standard 2-line smoothing with that obtained with the present 4-line strategy. For each test-case, one work unit is the time required by the best run. As shown in Figure 5, the 4-line smoothing provides very fast convergence (work ≈ 1) for a wide range of ε, using the maximum stable CFL number. Figure 5 also

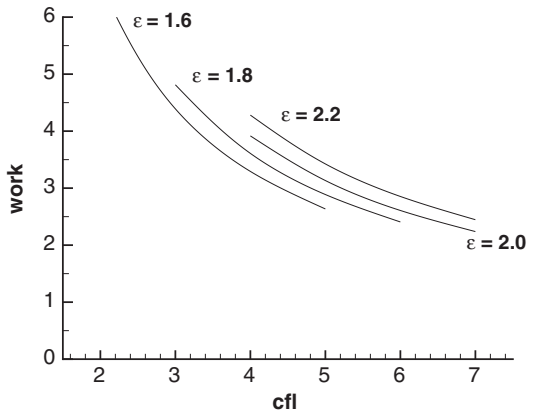

Figure 6. Channel flow: 2-line smoothing.

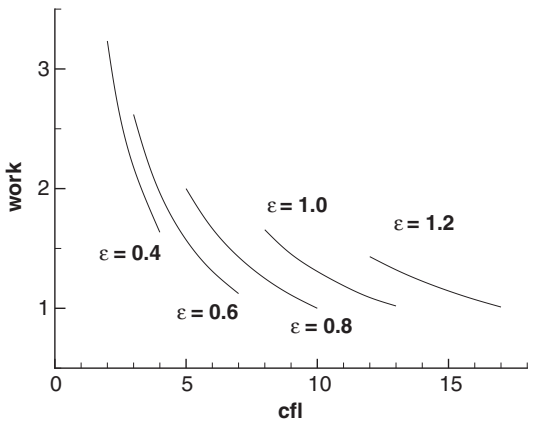

Figure 7. Subsonic airfoil: 4-line smoothing.

shows that a slight reduction of the CFL number improves the robustness, without affecting the efficiency significantly. When using only two smoothing lines, higher values of ε must be used, as expected; more importantly, the minimum CPU time is twice that required by the optimal 4-line runs (Figure 6). Similar results are obtained when comparing the best performances of the 2- and 4-line smoothings in the other three flow cases, and thus are not shown, for brevity. Figures 7–9 provide the results of an exhaustive application of the code to the single-grid solution of the three flows past the airfoil, using the 4-line smoothing only: the subsonic case behaves as the channel flow, with a very fast convergence for a wide range of ε, using the maximum stable CFL numbers (which are lower). A different behaviour appears in the transonic and in the laminar flow cases, where high local values of the flow residual are created while converging to steady state, namely, when the shocks begin to be

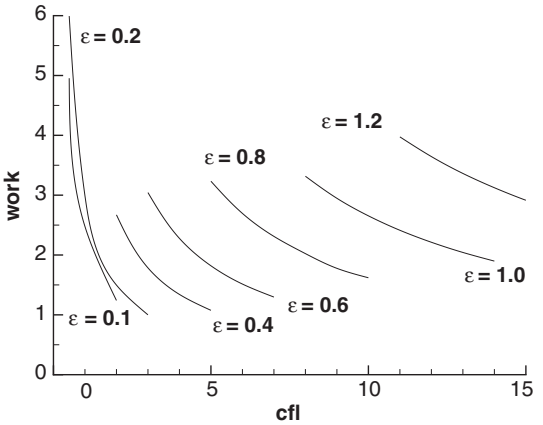

Figure 8. Transonic airfoil: 4-line smoothing.

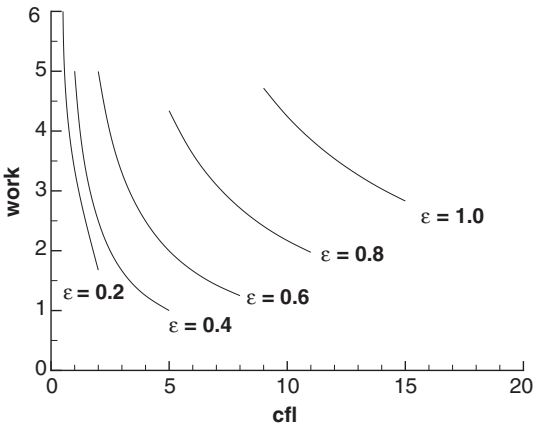

Figure 9. Laminar airfoil: 4-line smoothing.

sharpened or the recirculation region begins to be better defined: in such cases, an excessive smoothing leads to lower convergence rates, even allowing higher values of maximum stable CFL number.

Different optimal values of ε and CFL number have been found in the four test-cases analysed. However, a more careful examination of Figures 5, 7–9 shows that it is possible to choose constant values of ε and CFL number ($\varepsilon \approx 0.6$ and CFL ≈ 6.5), which are not optimal, but give fully satisfactory convergence rates in all test-cases considered.

The solution of the inviscid transonic flow past the NACA-0012 airfoil has been approached also using a standard MG strategy, which produces a further reduction of the CPU time by a factor of 4.5, as shown in Figure 10, which provides the convergence histories

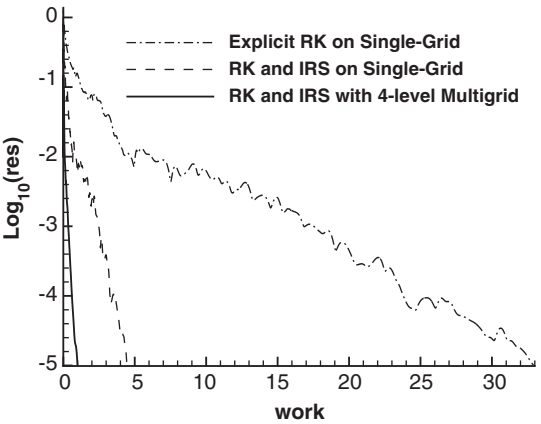

Figure 10. Transonic airfoil: convergence histories.

of two single-grid (without and with the optimal 4-line IRS) and of the optimal multigrid calculations.

6. CONCLUSIONS

A new line-search (LS) algorithm for cell-vertex unstructured triangular grids has been presented. Its combination with an IRS procedure has been widely tested versus inviscid and laminar flows through ducts and past airfoils. The proposed numerical results allow one to choose the optimal smoothing parameters and demonstrate that (i) the LS algorithm is cheap and robust and produces very good line patterns, which allow an efficient application of the standard IRS technique; (ii) for single-grid computations, a further significant improvement is obtained by using four smoothing directions, rather than the usual two; (iii) a very high efficiency of the 4-line IRS has been demonstrated also for multi-grid computations.

REFERENCES

1. Catalano LA. New reconstruction schemes for turbulent compressible flows on unstructured grids. *AIAA Paper 2001-2598*, *15th AIAA CFD Conference*, Anaheim, CA, U.S.A., 2001.
2. Catalano LA. A new reconstruction scheme for the computation of inviscid compressible flows on 3D unstructured grids. *International Journal for Numerical Methods in Fluids* 2002; **40**(1–2):273–279.
3. Catalano LA, Daloiso VSE. Accurate computation of 2D turbulent compressible flows on unstructured grids. *AIAA Paper 2003-3828*, *16th AIAA CFD Conference*, Orlando, FL, U.S.A., 2003.
4. Lerat A. Une classe de schémas aux différences implicites pour le sistémes hyperboliques de lois de conservation. *Comptes Rendus de l'Académie des Sciences Paris* 1979; **288A**:1033–1036.
5. Jameson A. The evolution of computational methods in aerodynamics. *Journal of Applied Mechanics Review* 1983; **50**(4b):1052–1070.
6. Roe PL. Characteristic based schemes for the Euler equations. *Annual Review of Fluid Mechanics* 1986; **18**:337–365.
7. Brandt A. Multi-level adaptive solutions to boundary-value problems. *Mathematics of Computation* 1977; **31**:333–390.

